
MODELLING TOROIDAL AND CYLINDRICAL DATA VIA THE TRIVARIATE WRAPPED CAUCHY COPULA WITH NON-UNIFORM MARGINALS

A PREPRINT

✉ **Sophia Loizidou**
University of Luxembourg
Luxembourg
sophia.loizidou@uni.lu

✉ **Christophe Ley**
University of Luxembourg
Luxembourg
christophe.ley@uni.lu

✉ **Shogo Kato**
Institute of Statistical Mathematics
Japan
skato@ism.ac.jp

✉ **Kanti V. Mardia**
University of Leeds
United Kingdom
k.v.mardia@leeds.ac.uk

November 14, 2025

ABSTRACT

In this paper, we propose a new flexible family of distributions for data that consist of three angles, two angles and one linear component, or one angle and two linear components. To achieve this, we equip the recently proposed trivariate wrapped Cauchy copula with non-uniform marginals and develop a parameter estimation procedure. We compare our model to its main competitors for analyzing trivariate data and provide some evidence of its advantages. We illustrate our new model using toroidal data from protein bioinformatics of conformational angles, and cylindrical data from climate science related to buoy in the Adriatic Sea. The paper is motivated by these real trivariate datasets.

Keywords Angular data · copula · directional statistics · flexible modeling

1 Introduction

Angular data are encountered in a wide range of disciplines, including environmental science (e.g., directions of wind or ocean waves), bioinformatics (such as dihedral angles in protein structures), zoology (tracking movement patterns of animals), medicine (e.g., circadian rhythms or hormone secretion timings), and the social or political sciences (for instance, the timing of crimes throughout the day); see, for example, [29]. Analyzing such data requires particular attention due to their inherent circular nature, typically defined on the interval $[0, 2\pi)$ with endpoints identified. This circular topology renders many standard statistical methods for real-valued data inapplicable or inadequate, implying the need to develop appropriate directional statistics methods [18, 34]. In particular, this has led to a plethora of new probability distributions for data consisting of one angle (circular case), two angles (toroidal case), and one angle and one linear component (cylindrical case), see for instance [29, Chapter 2], [35] and [39].

The situation is different when the data consists of either three angles, two angles and one linear component, or one angle and two linear components, where only a few proposals exist and most of them have problems of tractability, complex parameter estimation procedures, lack of practically usable random number generation or non-interpretable parameters (see Section 4). However, many such datasets exist which require an adequate statistical treatment. Two important examples are the following, which we will be analyzing with in this paper:

1. Protein data: Predicting the three-dimensional folding structure of a protein from its known one-dimensional amino acid structure is among the most important yet hardest scientific challenges, with impacts in drug development, vaccine design, disease mechanism understanding, human cell injection, and enzyme engineering, to cite but these. Demis Hassabis and John Jumper have been awarded the 2024 Nobel Prize in Chemistry for their deep learning based program AlphaFold which can predict protein structures with very good accuracy [42]; see also [31]. The recent Nature Methods paper [28] concretely stated the need to complement AlphaFold single point prediction with an adequate statistical uncertainty treatment: “distributions of conformations are the future of structural biology” (see our Section 5.1 for details). So far most statistical advances, in particular on flexible and tractable probability distributions, have considered the two dihedral angles ϕ and ψ , and considered the torsion angle of the side chain ω to be fixed at either 0 or π (which are the only two realistic values for this angle). One exception is [5] where ω is taken as binary random variable with value either 0 or π sampled using the hidden Markov model though the distribution is discrete not continuous. In practice, this angle ω is often measured with some noise, hence a joint model for all three angles ϕ , ψ and ω is required.
2. Climate data: Many environmental agencies are collecting data on wave heights and wave directions in order to identify sea regimes. Such identification is highly relevant in climate-change for studies of, for instance, the drift of floating objects and oil spills [16], coastal erosion [40], and the design of off-shore structures [8]; see [27] for further details. Typically, data analysis procedures use cylindrical distributions (e.g., the Abe–Ley distribution in [27]) to jointly model wave height and wave direction. A more scientifically strategic way is to add as additional variable the wind direction as it heavily influences waves in confined spaces. Quoting [27], “In wintertime, relevant events in the Adriatic Sea are typically generated by the southeastern Sirocco wind and the northern Bora wind”. That is, for such cases, we should add wind direction to the cylindrical data of wave height and wave direction used in [27]. Note that their aim is analyzing a time series of cylindrical data where the wind direction is not relevant. In our case we instead have three variables, wave height, wave direction and wind direction.

In the recent paper [24], we have proposed the trivariate wrapped Cauchy copula (TWCC) which precisely does satisfy the above-mentioned desiderata of tractability, good parameter estimation procedures, efficient random number generation and interpretable parameters. This copula can deal with three angles, yet it is itself not versatile enough because its marginals are uniform on the unit circle. Therefore, in this paper we propose an extension of the TWCC by adding general non-uniform marginal distributions to it, denoted TWCM for trivariate wrapped Cauchy copula with non-uniform marginals. Now, since the density of the uniform distribution on the circle exactly coincides with that of the uniform distribution on $[0, 1]$, our construction implies that linear marginals are also admissible, in order to also cover cylindrical data. Our extended model in this paper thus not only covers toroidal data but also cylindrical data, unlike the toroidal competitor models from the literature.

The paper is organized as follows. In Section 2 we review the trivariate wrapped Cauchy copula as proposed in [24]. In Section 3 we then introduce non-uniform marginals to the TWCC and hereby build the new flexible copula models TWCM, and we propose a parameter estimation procedure. A thorough comparison with the main competitors in the existing literature is given in Section 4, and in Section 5 the two real datasets described above are investigated by means of our methodology. Finally, Section 6 ends with a discussion and outlook on future research.

2 The trivariate wrapped Cauchy copula

In this section we will briefly recall the definition and main properties of the trivariate wrapped Cauchy copula (TWCC) of [24].

For $\mathbf{u} = (u_1, u_2, u_3)'$ and $\boldsymbol{\rho} = (\rho_{12}, \rho_{13}, \rho_{23})'$, the density of the TWCC is given by

$$t(\mathbf{u}; \boldsymbol{\rho}) = c_2 \left[c_1 + 2 \{ \rho_{12} \cos(u_1 - u_2) + \rho_{13} \cos(u_1 - u_3) + \rho_{23} \cos(u_2 - u_3) \} \right]^{-1}, \quad 0 \leq u_1, u_2, u_3 < 2\pi, \quad (1)$$

where $\rho_{12}, \rho_{13}, \rho_{23} \in \mathbb{R} \setminus \{0\}$, $\rho_{12}\rho_{13}\rho_{23} > 0$,

$$c_1 = \frac{\rho_{12}\rho_{13}}{\rho_{23}} + \frac{\rho_{12}\rho_{23}}{\rho_{13}} + \frac{\rho_{13}\rho_{23}}{\rho_{12}}, \quad (2)$$

and

$$c_2 = \frac{1}{(2\pi)^3} \left\{ \left(\frac{\rho_{12}\rho_{13}}{\rho_{23}} \right)^2 + \left(\frac{\rho_{12}\rho_{23}}{\rho_{13}} \right)^2 + \left(\frac{\rho_{13}\rho_{23}}{\rho_{12}} \right)^2 - 2\rho_{12}^2 - 2\rho_{13}^2 - 2\rho_{23}^2 \right\}^{1/2}. \quad (3)$$

Moreover, the parameters need to satisfy the condition that there exists one of the permutations of $(1, 2, 3)$, (i, j, k) , such that

$$|\rho_{jk}| < |\rho_{ij}\rho_{ik}|/(|\rho_{ij}| + |\rho_{ik}|), \quad (4)$$

where $\rho_{ji} = \rho_{ij}$ for $1 \leq i < j \leq 3$. If additionally they satisfy the identifiability constraint

$$\rho_{12}\rho_{13}\rho_{23} = 1, \quad (5)$$

then the parameters of the TWCC are identifiable (see [24] for the formal proof). Note that condition (4) can be re-expressed under simpler form as $\rho_{ij}^2\rho_{ik}^2 > (|\rho_{ij}| + |\rho_{ik}|)$ under (5). We will equivalently refer to this distribution as TWCC and $\text{TWCC}(\boldsymbol{\rho})$ in order to specify its parameters.

In the TWCC, different functions of the parameters ρ_{12}, ρ_{13} and ρ_{23} control the dependence between the U_i 's and the location of the modes, which have been well identified in [24]. An appealing aspect from a tractability and computational viewpoint is the closed form of the density which does not include integrals or infinite sums, unlike most of the existing distributions on the three-dimensional torus (see Section 4). Moreover, all conditional distributions are members of well-known families, such as the wrapped Cauchy distributions on the circle and the Kato–Pewsey distribution on the torus, and the bivariate marginals are bivariate wrapped Cauchy-type copulas. A simple random number generation algorithm and an efficient parameter estimation procedure via maximum likelihood estimation have been provided in [24].

3 Adding non-uniform marginals to the TWCC

Let $(U_1, U_2, U_3)'$ be a random vector which follows the $\text{TWCC}(\boldsymbol{\rho})$. For each $i = 1, 2, 3$, assume that either

- f_i is a density on the circle $[0, 2\pi)$ and F_i its distribution function with fixed and arbitrary origin, namely, $F_i(\theta) = \int_{c_i}^{\theta} f_i(x)dx$ with $c_i \in [0, 2\pi)$;
- f_i is a density on (a subset of) the real line \mathbb{R} and F_i its distribution function.

Define

$$(\Theta_1, \Theta_2, \Theta_3)' = \left(F_1^{-1} \left(\frac{U_1}{2\pi} \right), F_2^{-1} \left(\frac{U_2}{2\pi} \right), F_3^{-1} \left(\frac{U_3}{2\pi} \right) \right)'.$$

Then it follows that $(\Theta_1, \Theta_2, \Theta_3)'$ has the joint density

$$f(\boldsymbol{\theta}; \boldsymbol{\rho}) = (2\pi)^3 c_2 \left(c_1 + 2 \sum_{1 \leq i < j \leq 3} \rho_{ij} \cos[2\pi\{F_i(\theta_i) - F_j(\theta_j)\}] \right)^{-1} \prod_{1 \leq k \leq 3} f_k(\theta_k), \quad (6)$$

where $\boldsymbol{\theta} = (\theta_1, \theta_2, \theta_3)'$ and each θ_i either belongs to $[0, 2\pi)$ or to (a subset of) \mathbb{R} . We refer to this extension of $\text{TWCC}(\boldsymbol{\rho})$ with non-uniform marginals as TWCM. As is clear from the definition, the univariate marginal density of Θ_i is given by f_i ($i = 1, 2, 3$). This yields a very flexible class of distributions with either 3 angular components, 2 angular and 1 linear components, 1 angular and 2 linear components, or even 3 linear components.

The reason why there is no distinction between the type of marginals lies in the simple fact that the uniform distribution on $[0, 2\pi)$ bears by nature a double role as being linear as well as circular (since all points, and in particular the endpoints, share the same value). This unified viewpoint was not taken up by the two papers [21] and [44], of which the former introduced copulas for cylindrical data and the latter for toroidal data, nor in [22] where the concept of copulas for circular data has been discussed in general.

From the properties of $\text{TWCC}(\boldsymbol{\rho})$, we can derive general results about the distribution of the extended TWCC, such as conditional distributions. In the next theorem, whose proof is omitted (as it is similar to the proof of Theorems 2 and 3 of [24]), we give the marginal and conditional distributions of the TWCM.

Theorem 1. *Let $(\Theta_1, \Theta_2, \Theta_3)'$ follow TWCM with density (6). Then the following hold for $(\theta_1, \theta_2, \theta_3)'$ each either belonging to $[0, 2\pi)$ or to (a subset of) \mathbb{R} :*

- (i) *The univariate marginal distribution of Θ_i is $f_i(\theta_i)$.*
- (ii) *The bivariate marginal distribution of $(\Theta_i, \Theta_j)'$ is*

$$f(\theta_i, \theta_j) = 4\pi^2 t_2(2\pi F_i(\theta_i), 2\pi F_j(\theta_j); \phi_{ij}) f_i(\theta_i) f_j(\theta_j),$$

where, for $0 \leq u_i, u_j < 2\pi$, we define

$$t_2(u_i, u_j; \phi_{ij}) = \frac{1}{4\pi^2} \frac{|1 - \phi_{ij}^2|}{1 + \phi_{ij}^2 - 2\phi_{ij} \cos(u_i - u_j)}$$

with

$$\phi_{ij} = \frac{1}{2\rho_{ij}} \left\{ \frac{\rho_{ik}\rho_{jk}}{\rho_{ij}} - \frac{\rho_{ij}\rho_{ik}}{\rho_{jk}} - \frac{\rho_{ij}\rho_{jk}}{\rho_{ik}} - (2\pi)^3 c_2 \right\}, \quad (7)$$

and c_2 is as in (3).

(iii) The bivariate conditional distribution of $(\Theta_i, \Theta_j)'$ given $\Theta_k = \theta_k$ is

$$f(\theta_i, \theta_j | \theta_k) = 4\pi^2 t_{2|1}(2\pi F_i(\theta_i), 2\pi F_j(\theta_j) | 2\pi F_k(\theta_k); \boldsymbol{\rho}) f_i(\theta_i) f_j(\theta_j),$$

where, for $0 \leq u_i, u_j, u_k < 2\pi$, we have

$$t_{2|1}(u_i, u_j | u_k; \boldsymbol{\rho}) = 2\pi c_2 \left[c_1 + 2 \{ \rho_{ij} \cos(u_i - u_j) + \rho_{ik} \cos(u_i - u_k) + \rho_{jk} \cos(u_j - u_k) \} \right]^{-1}.$$

(iv) The univariate conditional distribution of Θ_i given $\Theta_j = \theta_j$ is

$$f(\theta_i | \theta_j) = 2\pi t_{1|1}(2\pi F_i(\theta_i) | 2\pi F_j(\theta_j); \phi_{ij}) f_i(\theta_i),$$

where, for $0 \leq u_i, u_j < 2\pi$, we define

$$t_{1|1}(u_i | u_j; \phi_{ij}) = \frac{1}{2\pi} \frac{|1 - \phi_{ij}^2|}{1 + \phi_{ij}^2 - 2\phi_{ij} \cos(u_i - u_j)}$$

with ϕ_{ij} given in (7).

(v) The univariate conditional distribution of Θ_i given $(\Theta_j, \Theta_k)' = (\theta_j, \theta_k)'$ is

$$f(\theta_i | \theta_j, \theta_k) = 2\pi t_{1|2}(2\pi F_i(\theta_i) | 2\pi F_j(\theta_j), 2\pi F_k(\theta_k); \delta_{i|jk}) f_i(\theta_i),$$

where, for $0 \leq u_i, u_j, u_k < 2\pi$, we define

$$t_{1|2}(u_i | u_j, u_k; \eta_{i|jk}, \delta_{i|jk}) = \frac{1}{2\pi} \frac{|1 - \delta_{i|jk}^2|}{1 + \delta_{i|jk}^2 - 2\delta_{i|jk} \cos(u_i - \eta_{i|jk})}$$

with $\eta_{i|jk} = \arg(\phi_{i|jk})$ and $\delta_{i|jk} = |\phi_{i|jk}|$ for $\phi_{i|jk} = -\rho_{jk}^{-1} e^{iu_j} + \rho_{ij}^{-1} e^{iu_k}$.

The results demonstrate that with our extended model all forms of regression analysis involving up to three angular and/or linear components are straightforward, which in a unified way covers what we described as our objective in Section 1. Random number generation from TWCM is also immediate by adding just the step

$$\Theta_i = F_i^{-1} \left(\frac{U_i}{2\pi} \right), \quad i = 1, 2, 3,$$

to the algorithm presented for the TWCC in [24].

The parameters of the extended TWCC as in (6) are estimated using MLE. When the marginals are uniform, the procedure from [24] applies. In the case that the marginal distributions are not uniform, the maximum likelihood estimates of the parameters are calculated in a two-step approach. Let $\{(\theta_{1m}, \theta_{2m}, \theta_{3m})'\}_{m=1}^n$ denote the sequence of toroidal observations from (6). In the first step, the ML estimates of the parameters of the marginals are calculated, followed in the second step by estimating the parameters of the copula using $\{(u_{1m}, u_{2m}, u_{3m})'\}_{m=1}^n$ for

$$(u_{1m}, u_{2m}, u_{3m})' = \left(2\pi F_1(\theta_{1m}; \hat{\nu}_1), 2\pi F_2(\theta_{2m}; \hat{\nu}_2), 2\pi F_3(\theta_{3m}; \hat{\nu}_3) \right)',$$

where, for $i \in \{1, 2, 3\}$, F_i represents the marginal density function of θ_i and $\hat{\nu}_i$ the parameters of F_i obtained from the first step of the maximization. [19] refers to this as the method of inference functions for marginals or IFM method. Efficiency and consistency of the estimates obtained with IFM compared to the estimates that can be obtained by performing one maximisation of the likelihood function can be found in [19, Chapter 10] and [20, Chapter 5].

We conclude this section by briefly discussing one important choice of univariate marginals as in Theorem 1(i), namely when each f_i is the wrapped Cauchy density

$$f_i(\theta) = \frac{1}{2\pi} \frac{1 - \xi_i^2}{1 + \xi_i^2 - 2\xi_i \cos(\theta - \mu_i)}, \quad 0 \leq \theta < 2\pi, \quad (8)$$

where μ_i is the location parameter and $\xi_i \in (-1, 1)$ the concentration parameter. Assume that the origin of the distribution function F_i is $c_i = \mu_i$. In this case F_i has the closed-form expression

$$F_i(\theta_i) = \frac{1}{\pi} \arctan \left(\frac{1 + \xi_i}{1 - \xi_i} \tan \frac{\theta_i - \mu_i}{2} \right) + I(\theta_i > \mu_i + \pi), \quad \mu_i < \theta_i < \mu_i + 2\pi.$$

Then, noting that $\cos(2 \arctan x) = (1 - x^2)/(1 + x^2)$ and $\sin(2 \arctan x) = 2x/(1 + x^2)$, $x \in \mathbb{R}$, it can be shown that the density of (6) can be expressed as

$$f(\boldsymbol{\theta}; \boldsymbol{\rho}) = c_2 \prod_{i=1}^3 (1 - \xi_i^2) \left[c_1 \prod_{i=1}^3 g_i(\theta_i) + 2 \sum_{\substack{1 \leq j < k \leq 3 \\ i \neq j, k}} \rho_{ij} g_k(\theta_k) h_{ij}(\theta_i, \theta_j) \right]^{-1}, \quad (9)$$

where $g_i(\theta_i) = 1 + \xi_i^2 - 2\xi_i \cos(\theta_i - \mu_i)$ and

$$\begin{aligned} h_{ij}(\theta_i, \theta_j) &= (1 + \xi_i^2)(1 + \xi_j^2) \cos(\theta_i - \mu_i) \cos(\theta_j - \mu_j) \\ &\quad + (1 - \xi_i^2)(1 - \xi_j^2) \sin(\theta_i - \mu_i) \sin(\theta_j - \mu_j) - 2\xi_j(1 + \xi_i^2) \cos(\theta_i - \mu_i) \\ &\quad - 2\xi_i(1 + \xi_j^2) \cos(\theta_j - \mu_j) + 4\xi_i \xi_j. \end{aligned}$$

Note that the density (9) does not involve any integrals. As further nice properties derived from Theorem 1, the wrapped Cauchy copula with wrapped Cauchy marginals also has wrapped Cauchy conditionals for Θ_i given $\Theta_j = \theta_j$ and for Θ_i given $(\Theta_j, \Theta_k)' = (\theta_j, \theta_k)'$. Moreover, the bivariate marginal distribution of $(\Theta_i, \Theta_j)'$ is the bivariate wrapped Cauchy distribution of [25] with density

$$\begin{aligned} f(\theta_i, \theta_j) &= \tilde{\gamma} \{ \tilde{\gamma}_0 - \tilde{\gamma}_1 \cos(\theta_i - \mu_i) - \tilde{\gamma}_2 \cos(\theta_j - \mu_j) - \tilde{\gamma}_3 \cos(\theta_i - \mu_i) \cos(\theta_j - \mu_j) \\ &\quad - \tilde{\gamma}_4 \sin(\theta_i - \mu_i) \sin(\theta_j - \mu_j) \}^{-1}, \end{aligned}$$

where $\tilde{\gamma} = (1 - \rho_{ij}^2)(1 - \xi_i^2)(1 - \xi_j^2)/(4\pi^2)$, $\tilde{\gamma}_0 = (1 + \rho_{ij}^2)(1 + \xi_i^2)(1 + \xi_j^2) - 8\rho_{ij}\xi_i\xi_j$, $\tilde{\gamma}_1 = 2(1 + \rho_{ij}^2)\xi_i(1 + \xi_j^2) - 4\rho_{ij}(1 + \xi_i^2)\xi_j$, $\tilde{\gamma}_2 = 2(1 + \rho_{ij}^2)(1 + \xi_i^2)\xi_j - 4\rho_{ij}\xi_i(1 + \xi_j^2)$, $\tilde{\gamma}_3 = -4(1 + \rho_{ij}^2)\xi_i\xi_j + 2\rho_{ij}(1 + \xi_i^2)(1 + \xi_j^2)$, and $\tilde{\gamma}_4 = 2\rho_{ij}(1 - \xi_i^2)(1 - \xi_j^2)$. Random number generation from the distribution (9) can be carried out using the Möbius transformation

$$\Theta_i = F_i^{-1} \left(\frac{U_i}{2\pi} \right) = \mu_i + 2 \arctan \left[\frac{1 - \xi_i}{1 + \xi_i} \tan \left(\frac{U_i}{2} \right) \right].$$

4 Main competitors from the literature

Having discussed the main properties of our new TWCM, we can now proceed to a discussion of its main competitors from the literature. Bearing in mind that this is the first paper on trivariate copulas for both angular and cylindrical data, its competitors are in the angular (toroidal) case only.

There is a d -dimensional toroidal copula model of importance given in [26]. Its construction is very general, but no code for its application is provided. The authors have performed a comparison of distinct models based on trivariate angular protein data and have come to the conclusion that, in terms of AIC, the multivariate nonnegative trigonometric sums (MNNTS) model of [9] is the best choice when $d = 3$. The probability density function of the MNNTS is given by

$$f(\theta_1, \theta_2, \dots, \theta_d) = \sum_{k_1=0}^{M_1} \sum_{k_2=0}^{M_2} \cdots \sum_{k_d=0}^{M_d} \sum_{m_1=0}^{M_1} \sum_{m_2=0}^{M_2} \cdots \sum_{m_d=0}^{M_d} c_{k_1 k_2 \dots k_d} \bar{c}_{m_1 m_2 \dots m_d} e^{\sum_{s=1}^d i(k_s - m_s)\theta_s} \quad (10)$$

where $c_{k_1 k_2 \dots k_d}$ and $\bar{c}_{m_1 m_2 \dots m_d}$ are the parameters with \bar{c} the complex conjugate of c . Based on the findings from [26], we will just focus on this model when analyzing protein data in Section 5.1.

The paper [26] also considers the well-established multivariate von Mises distribution of [33] which again does not do as well for that dataset though this model belongs to the exponential family so inherits several desirable properties of this family.

There are other choices such as the multivariate Generalised von Mises (mGvM) distribution [38], the multivariate wrapped normal distribution [3], the multivariate projected normal distribution [37], and the inverse stereographic normal distribution [41], but these all have some limitations in comparison to our model such as either their normalizing constants are intractable so the MLE computations are not easy, they may be multimodal, or sampling is not clear-cut. Hence, we have selected only the MNNTS as competitor in Section 5.1 for our protein data.

5 Practical applications

5.1 Protein data

As mentioned in Section 1, an essential challenge in the prediction of the 3D structure of proteins is the ability to jointly model the conformational angles ϕ, ψ (dihedral angles) and ω (torsion angle of the side chain). The main body of statistical research in this direction has so far concentrated on the two conformational angles ϕ, ψ , which has already led to important contributions in the protein structure prediction problem, see for example [5], [15], [11], [14], and Chapters 1 and 4 of [29]. This is due to the fact that, theoretically, the torsion angle ω is either 0 or π radians, corresponding to peptide planarity. However, [4] have investigated this issue in detail and shown that peptide planarity is not a common feature for collected data. In their paper, they conduct an exploratory data analysis of all three conformational angles. The authors from [36], [33] and [26] have modelled three or more angles with their proposed distributions. The main problem of statistical approaches to protein structure prediction is that they are computationally intensive (especially due to intricate normalizing constants), and we believe that our proposal, which is a faster method, can make the statistical approach more feasible.

We now give some background to protein structure. The building blocks of proteins are the amino acids, which consist of the backbone and the sidechains. The backbone consists of the chemical bonds NH- C_α and C_α -CO, where C_α denotes the central Carbon atom. These bonds can rotate around their axes, with ϕ denoting the NH- C_α angle and ψ the C_α -CO angle. These angles need to be studied as specific combinations of them allow the favourable hydrogen bonding patterns, while others can ‘result in clashes within the backbone or between adjacent sidechains’ [17, 30, 32]. The ω angle denotes the N-C torsion angle, where C is the non-central carbon atom. As we have said before, theoretically the angle ω can only take the values 0 and π , and in some of the research work, this angle was fixed at one of the two values [2, 15]. However, in practice this angle is often measured with some noise and using our extended TWCC, we shall model all three angles. In bioinformatics, and as already mentioned, all three angles are studied in [4] and we will give some comments on how their exploratory work is explained by our model.

For the present data analysis, we consider position 55 at 2000 randomly selected times in the molecular dynamic trajectory of the SARS-CoV-2 spike domain from [13]. The position occurs in α -helix throughout the trajectory. DPPS [23] is used to compute the secondary structure and [7] to verify the chains. As can be seen from Figure 1, the marginal distributions of the angles ϕ, ψ and ω for this dataset cannot well be modelled by the uniform distribution on the circle (as done in [24]), so other distributions need to be explored. We combined the TWCM with wrapped Cauchy, cardioid, von Mises and Kato–Jones marginals. Of course, many other choices are possible, and one can also combine distinct marginals. Whatever marginals we choose, the parameters of our models are estimated using MLE (IFM) as explained in Section 3 and a model comparison is carried out using the Akaike Information Criterion (AIC) and the Bayesian Information Criterion (BIC).

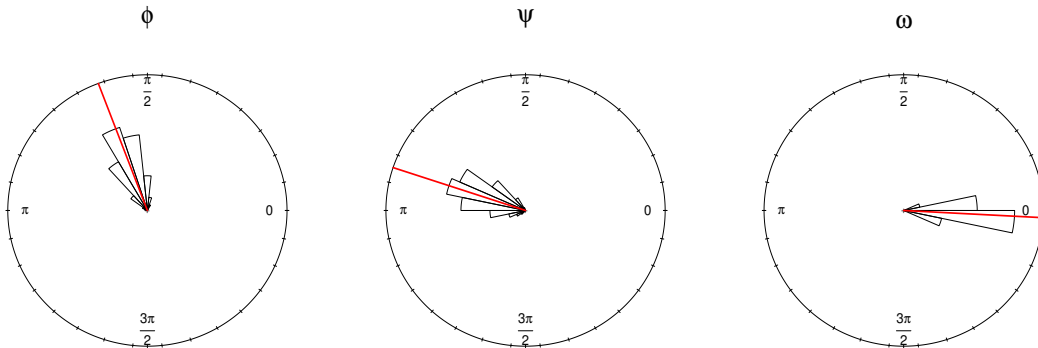


Figure 1: Rose plots of the protein data for the three angles ϕ, ψ, ω . The marginals are not uniformly distributed on the circle. The mean direction, calculated using von Mises marginals, is plotted in red.

Table 1: Maximized log-likelihood, AIC, BIC, and the number of free parameters (denoted by p) for the two models (TWCM and MNNTS) for the protein dataset.

Model	Marginals	log-likelihood	AIC	BIC	p
TWCM	uniform	-7920	15843	15855	2
	wrapped Cauchy	1131	-2247	-2202	8
	cardioid	-3495	7005	7050	8
	von Mises	2046	-4076	-4031	8
	Kato–Jones	1395	-2762	-2684	14
(M_1, M_2, M_3)					
MNNTS	(0,0,0)	-11027	22055	22055	0
	(1,1,1)	-6923	13874	13953	14
	(2,2,2)	-4582	9268	9559	52
	(3,3,3)	-2984	6220	6926	126
	(4,4,4)	-1811	4118	5507	248
	(5,5,5)	-921	2702	5111	430
	(6,6,6)	-231	1829	5660	684
	(7,7,7)	315	1414	7138	1022

As conditional plots of two angles given one turn out to be informative in our setting, Figure 2 shows the plots of the data of two of the angles given the third one. The values of the fixed angles in radians ($\phi = 1.93$, $\psi = 2.8$ and $\omega = 0$) are chosen to be the mode of the data, and only points that are within 0.1 radians of the selected value of the fixed angle are plotted. In order to make the plots clearer, the range of values on each axis is not between 0 and 2π , like the traditional Ramachandran plot, but it is chosen such that both the contour plots and the points are visible (in summary, we have re-scaled the plots). For the values of ω , most observations were around 0 and so the plot is translated from $[0, 2\pi)$ to $[-\pi, \pi)$ in order to be able to make the range of values shown on the axis smaller and hence the presentation clearer. The contour plots correspond to our copula density (1) with the marginal distributions being the von Mises distribution, whose density is given by

$$f(\theta) = \frac{1}{2\pi I_0(\kappa)} \exp^{\kappa \cos(\theta - \mu)}, \quad \theta \in [0, 2\pi), \quad (11)$$

where $I_0(\kappa)$ denotes the modified Bessel function of the first kind and order 0. The von Mises marginals with their lighter tails lead to the best fit for this concentrated dataset, as measured by both AIC and BIC, see Table 1. The observed data points are plotted on top of the contours. This gives a visual indication of how good our estimated model fits this protein dataset.

For TWCM with von Mises marginals, the standard errors of the estimated parameters can be evaluated by means of bootstrap. Using $B = 1000$ bootstrap samples, the maximum likelihood estimates of the parameters, with the standard error given in parenthesis, are $\hat{\rho}_{12} = 9.18(4.99)$, $\hat{\rho}_{13} = -1.17(4.60)$, $\hat{\rho}_{23} = -0.09(4.41)$ for the copula parameters and $\hat{\mu}_1 = 1.93(0.0043)$, $\hat{\kappa}_1 = 27.6(0.99)$, $\hat{\mu}_2 = 2.82(0.0055)$, $\hat{\kappa}_2 = 17.3(0.62)$, $\hat{\mu}_3 = 6.23(0.0024)$, $\hat{\kappa}_3 = 84.4(2.95)$, where $\hat{\mu}_i$ and $\hat{\kappa}_i$ denote the estimated values for μ and κ of density (11) corresponding to the marginal distribution of θ_i for $i \in \{1, 2, 3\}$. We attribute the relatively high standard errors of the copula parameters to the condition (5) which links all three parameters.

Our findings regarding the angle ω confirm the exploratory analysis done by [4]: the data points are strongly concentrated around the modal direction $\hat{\mu}_3$, but are not exactly equal to that value, as can also be visually appreciated from the plot in Figure 1. The inherent tractability of our model allows biologists and bioinformaticians to quantify uncertainties, compute quantities of interest, and in particular our straightforward random number generation process enables them to quickly simulate data from our model, which is essential in their pipelines [43].

We conclude this section by a comparison of our model with the MNNTS distribution (10) of [9] which we summarized in Section 4. Table 1 presents the fit of various models. The maximised log-likelihood, AIC and BIC are reported for each model, along with the number of free parameters, denoted by p . The algorithms for fitting the MNNTS distribution are taken from the R package CircNNTSR [10]. Besides the reasons mentioned in Section 4 to compare our model to the MNNTS, it is also the only competitor for which we could find implemented and working code. The number of free parameters for $\text{MNNTS}(M_1, M_2, M_3)$ is calculated as $2 \left(\prod_{i=1}^3 (M_i + 1) - 1 \right)$. Various combinations of the values M_1, M_2, M_3 are shown in Table 1, with the number of free parameters increasing rapidly. The MNNTS is not able to match the fit of our copula (not only in terms of AIC/BIC but even in terms of log-likelihood), even for a very large number of parameters. The best model for all three measures of fit, the trivariate wrapped Cauchy copula with von Mises marginals, is shown in bold.

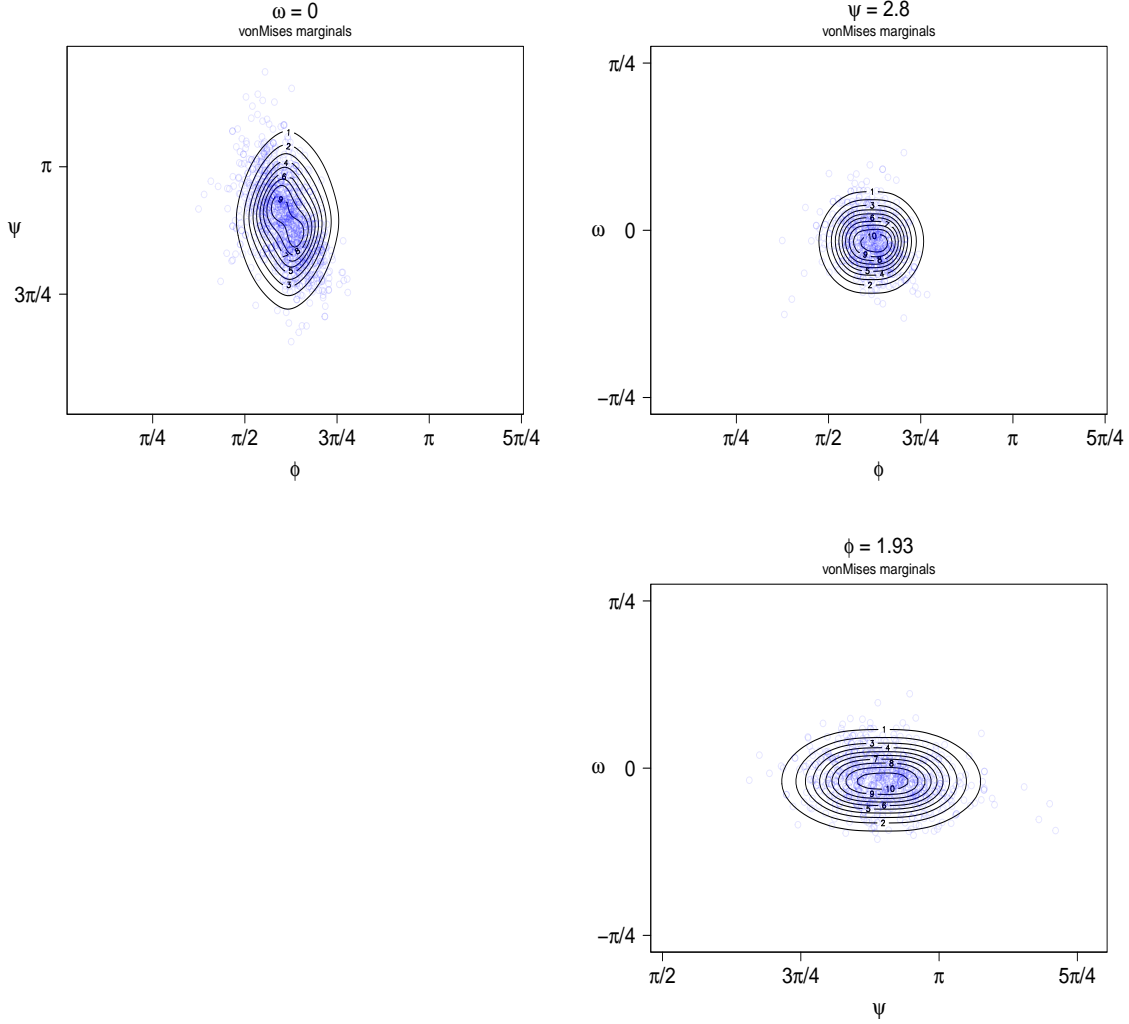


Figure 2: Contour plots of TWCM with von Mises marginals, with parameter values estimated by maximum likelihood (IFM). The parameters of the marginals are $\hat{\mu}_1 = 1.93$, $\hat{\kappa}_1 = 27.6$, $\hat{\mu}_2 = 2.82$, $\hat{\kappa}_2 = 17.3$, $\hat{\mu}_3 = 6.23$, $\hat{\kappa}_3 = 84.4$, where $\hat{\mu}_i$ and $\hat{\kappa}_i$ denote the estimated value for μ and κ of density (11) corresponding to the marginal distribution of θ_i for $i \in \{1, 2, 3\}$, and the copula parameters are $\hat{\rho}_{12} = 9.18$, $\hat{\rho}_{13} = -1.17$, $\hat{\rho}_{23} = -0.09$.

5.2 Climate data

As discussed in the Introduction, the joint modeling of wave height and wave direction is a common approach in environmental studies aiming to identify sea regimes, with applications ranging from coastal erosion to offshore engineering and pollution tracking. Cylindrical distributions, such as the Abe–Ley distribution [1], are typically employed for this purpose. However, as previously emphasized, a more comprehensive analysis requires the inclusion of wind direction, which plays a critical role in shaping wave patterns, particularly in semi-enclosed basins. This is especially relevant in regions like the Adriatic Sea, where seasonal winds such as the Sirocco and Bora significantly influence wave dynamics [27]. In the following, we analyze a dataset that captures this triplet structure, that is, wave height (linear, x) and direction (circular, θ_1), as well as wind direction (circular, θ_2). Such data thus is on a hyper-cylinder, which we can analyze with our copula.

For this purpose we use a time series of 1326 observations of red half-hourly wave directions and heights as well as wind directions, recorded in the period 15/02/2010 – 16/03/2010 by the buoy of Ancona, located in the Adriatic Sea at about 30 km from the coast. The data points are collected far spaced enough from each other to be considered independent. We choose as our circular marginals the wrapped Cauchy distribution (8) and the Weibull distribution for the linear marginal, with density given by

$$f(x) = \frac{\nu}{\lambda} \left(\frac{x}{\lambda}\right)^{\nu-1} \exp^{-(x/\lambda)^\nu},$$

where ν is the shape parameter and λ is the scale parameter. Of course, many other combinations could be considered, but these work as we see. Our exploratory analysis shows that our data is multimodal and hence a mixture model is required, so we use densities of the form

$$f(\theta_1, \theta_2, x) = \sum_{i=1}^K \pi_i f_i(\theta_1, \theta_2, x), \quad \sum_{i=1}^K \pi_i = 1, \quad (12)$$

where K is the number of components of the mixture model, π_i is the weight of each class $i = 1, \dots, K$ and $f_i(\theta_1, \theta_2, x)$ is the density of component i and is the copula as defined in (6), with marginals as already explained. In order to estimate the parameters, we use a variant of the Expectation-Maximization (EM) algorithm to find the values of the parameters for each component of the mixture model. As with maximum likelihood estimation with non-uniform marginals, the maximisation is done as a first step for the parameters of the marginal distributions and then, using the obtained parameters, estimates of the parameters of the copula are obtained. The M-step of our algorithm thus adopts the IFM method described in Section 3, which is why we speak of a variant of the EM algorithm, which for the rest works exactly like an EM algorithm. The initial values for the parameters were randomly chosen. This was repeated 10 times and the parameters that maximised the log-likelihood were chosen. To find the number of mixture components, we considered the values $K = 2, 3, 4, 5$ and used the BIC to determine the best-fitting model. We found that $K = 4$ components fit best the data, as the BIC values are 16045, 15850, 10750 and 15655, for $K = 2, 3, 4, 5$, respectively.

We now give the parameter estimates, plots of the data and clusters, and analyse the data based on our copula. The parameter estimates for this mixture model are given in Table 2. It should be noted that in each of the clusters, one of the ρ_{ij} is large in absolute value, meaning that we are in the limit case discussed in [24]. The values of the ρ_{ij} s are very different between each cluster, with Cluster 3 having a very large negative value for $\hat{\rho}_{12}$, Cluster 1 having a smaller negative value for the same parameter and Cluster 2 having a large positive value for $\hat{\rho}_{13}$. The values of the parameters calculated for Cluster 4 are not as extreme. For visualization of the results, the bivariate marginal distribution is plotted in Figure 3, as given in Theorem 1, with N, E, S, W representing north, east, south and west, respectively. The plots on the left hand side are scatter plots of the data, coloured according to their cluster as given by our variant of the EM algorithm with 4 components. The same colour is used for each cluster to plot the bivariate marginal distribution for each of the components. In the Adriatic sea, the predominant winds are bora, coming from north/north-east, and sirocco, from the south-east. The different winds are captured in different clusters of the data, with the red and green cluster being caused by the bora wind and dark blue by the sirocco wind.

6 Future research

The flexibility of the TWCM allows for several applications of the distribution, as well as further extensions. Regarding protein structure prediction, the methodology of the seminal paper [6] uses a trivariate distribution with ω as discrete variable in their software TorusDBN and in the future it would be worth investigating if using the TWCM instead of their trivariate distribution leads to any improvement in prediction.

We now discuss a few extensions. First, we might wish to introduce asymmetry into our copula TWCC(ρ). Skewness can be handled at the level of the marginals via suitably choosing skew marginal distributions, but this does not allow

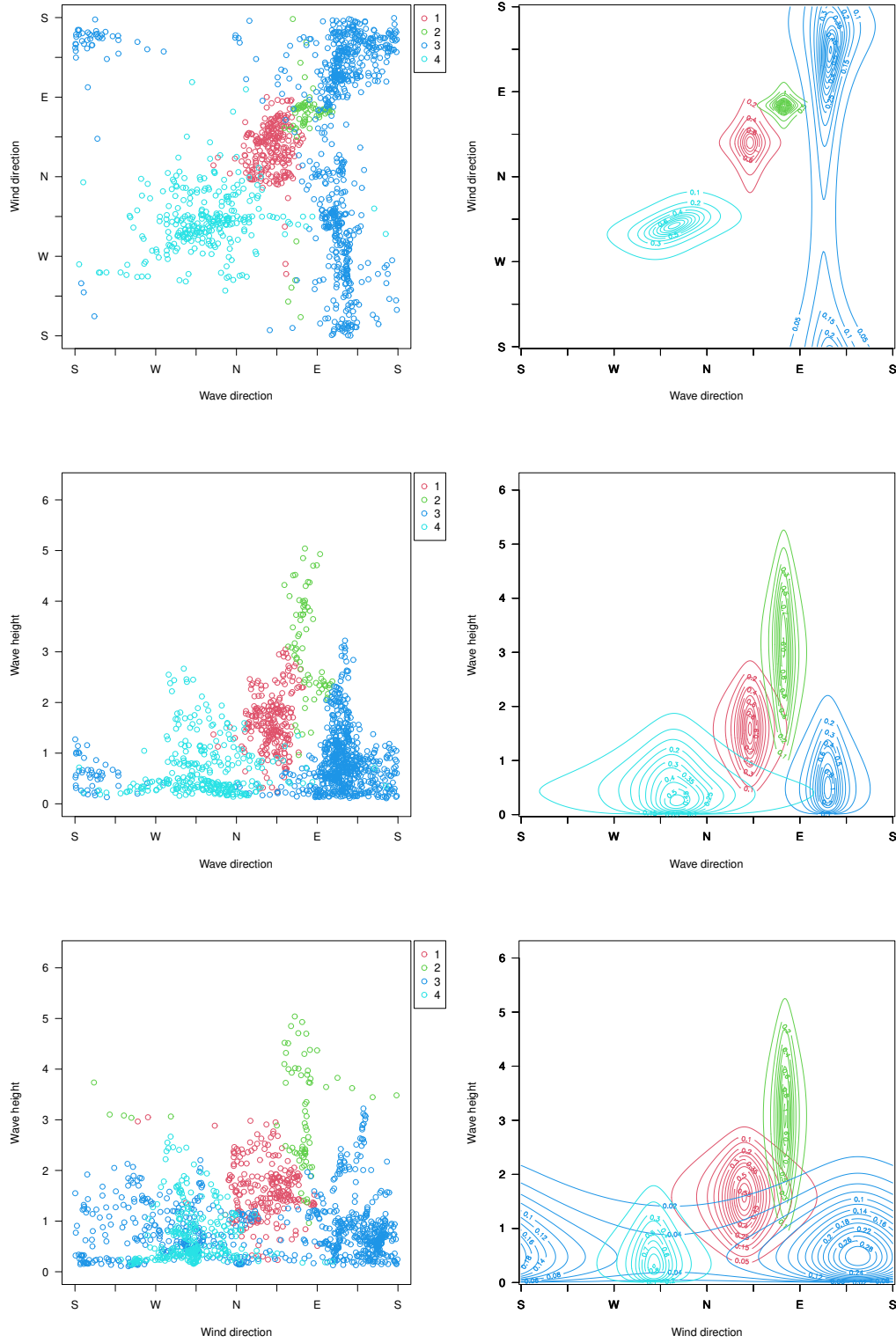


Figure 3: Contour plots for the climate data of the bivariate marginal distributions of our extended TWCC for the four different clusters as detected by our variant of the EM algorithm. Each cluster is presented in a different colour and N, E, S, W represent north, east, south and west, respectively.

Table 2: Parameter estimates as obtained from our variant of the EM algorithm for 4 components. The marginal distributions for wind and wave directions are wrapped Cauchy, and the estimates of the parameters are denoted by $\hat{\xi}_1, \hat{\mu}_1$ and $\hat{\xi}_2, \hat{\mu}_2$, respectively, with π representing north. For the wave height we use the Weibull distribution, where $\hat{\lambda}_3$ is the estimated scale parameter and $\hat{\nu}_3$ the estimated shape parameter. Finally $\hat{\pi}_i$ denotes the estimate of the weight of class i .

Parameters	Cluster 1	Cluster 2	Cluster 3	Cluster 4
$\hat{\rho}_{12}$	-92.092	-0.008	-5956.914	-5.168
$\hat{\rho}_{13}$	43.331	584.384	-0.032	0.864
$\hat{\rho}_{23}$	-0.0003	-0.218	0.005	-0.224
$\hat{\mu}_1$	3.869	4.440	5.184	2.588
$\hat{\xi}_1$	0.834	0.882	0.809	0.578
$\hat{\mu}_2$	3.772	4.460	5.692	2.239
$\hat{\xi}_2$	0.729	0.887	0.432	0.736
$\hat{\lambda}_3$	1.781	3.414	0.948	0.766
$\hat{\nu}_3$	3.207	3.390	1.531	1.424
$\hat{\pi}_i$	0.184	0.054	0.546	0.216

altering the symmetry of the dependence structure, hence the copula itself. For example, this can be done by adopting the approach of [2] which consists in multiplying (1) with the skewing function $(1 + \lambda_1 \sin(u_1) + \lambda_2 \sin(u_2) + \lambda_3 \sin(u_3))$ for $\lambda_1, \lambda_2, \lambda_3 \in (-1, 1)$ satisfying $|\lambda_1| + |\lambda_2| + |\lambda_3| < 1$. When all three skewness parameters are 0, we retrieve the original copula, and as soon as one parameter deviates from zero, we obtain a skew version of our TWCC(ρ) given by (1). As future work, it will be interesting to see in how far asymmetry in the copula can add flexibility on top of asymmetry in the marginals, and how both can be ideally combined.

Second, in a similar manner as in [44], the TWCM can be used to construct an AR(2) process on the circle. Let $\Theta_0, \Theta_1, \dots$, be $[0, 2\pi)$ -valued random variables on the circle such that

$$p(\theta_0, \theta_1) = f(\theta_0, \theta_1),$$

$$p(\theta_t | \theta_{t-1}, \dots, \theta_0) = p(\theta_t | \theta_{t-1}, \theta_{t-2}) = \frac{|1 - \delta_t^2|}{1 + \delta_t^2 - 2\delta_t \cos(2\pi F(\theta_t) - \eta_t)} f(\theta_t), \quad t = 2, 3, \dots, \quad (13)$$

where $p(\theta_0, \theta_1)$ is the initial distribution and $p(\theta_t | \theta_{t-1}, \theta_{t-2})$ is the transition density. Here $f(\theta_t)$ is a density on the circle $[0, 2\pi)$, $F(\theta_t) = \int_c^{\theta_t} f(x) dx$ for some arbitrary origin c on the circle, and $f(\theta_0, \theta_1)$ is a density on the torus $[0, 2\pi)^2$ with a common univariate marginal density f . Also, the parameters are assumed to satisfy $\eta_t = \arg(\phi_t)$, $\delta_t = |\phi_t|$, $\phi_t = -\rho_{t-1, t-2} \{ \rho_{t, t-1}^{-1} e^{2\pi i F(\theta_{t-1})} + \rho_{t, t-2}^{-1} e^{2\pi i F(\theta_{t-2})} \}$, $\rho_{t, t-1}, \rho_{t, t-2}, \rho_{t-1, t-2} \in \mathbb{R}$, $\rho_{t, t-1} \cdot \rho_{t, t-2} \cdot \rho_{t-1, t-2} > 0$, and $|\rho_{jk}| < |\rho_{ij} \rho_{ik}| / (|\rho_{ij}| + |\rho_{ik}|)$ for (i, j, k) a permutation of $(t, t-1, t-2)$. The transition density (13) is derived by substituting $(\theta_t, \theta_{t-1}, \theta_{t-2})$ into $(\theta_1, \theta_2, \theta_3)$ in (6) with the common marginal density f and calculating its univariate conditional density. Hence, it is clear that this circular AR(2) process $\{\Theta_i\}$, under the conditions above, is strictly stationary in the sense that $(\Theta_{t_1+\tau}, \dots, \Theta_{t_n+\tau}) \stackrel{d}{=} (\Theta_{t_1}, \dots, \Theta_{t_n})$ for any nonnegative integers t_1, \dots, t_n, τ and any positive integer n . If f is the wrapped Cauchy density (8), then the transition density (13) can also be expressed in closed form without integrals. The tractability of our model would make the circular AR(2) process very appealing and important for time-dependent directional data.

We also mention that a general d -dimensional extension of the TWCM follows in the same way as the d -dimensional generalization of the TWCC in [24] by again extending the uniform marginals to any marginals. Moreover, as alternative to the TWCM one could estimate the marginals in a non-parametric way and then combine the estimated marginals with our TWCC (see [12] for such a procedure in \mathbb{R}^d).

Code availability: The relevant code of the paper is available in <https://doi.org/10.5281/zenodo.15675162> as well as in <https://github.com/Sophia-Loizidou/Trivariate-wrapped-Cauchy-copula>.

Acknowledgements: The authors would like to thank Thomas Hamelryck and Ola Rønning for the protein data. Kanti Mardia would like to thank the Leverhulme Trust for the Emeritus Fellowship.

Funding: Shogo Kato was supported by JSPS KAKENHI Grant Number 20K03759 and 25K15037. Sophia Loizidou was supported by the grant PRIDE/21/16747448/MATHCODA from the Luxembourg National Research Fund.

References

- [1] T. Abe and C. Ley. A tractable, parsimonious and flexible model for cylindrical data, with applications. *Economics and Statistics*, 4:91–104, 2017.
- [2] J. Ameijeiras-Alonso and C. Ley. Sine-skewed toroidal distributions and their application in protein bioinformatics. *Biostatistics*, 23:685–704, 2022.
- [3] Y. Baba. Statistics of angular data: wrapped normal distribution model (in japanese). *Proceedings of the Institute of Statistical Mathematics*, 28:41–54, 1981.
- [4] D. S. Berkholz, C. M. Driggers, M. V. Shapovalov, R. L. Dunbrack Jr, and P. A. Karplus. Nonplanar peptide bonds in proteins are common and conserved but not biased toward active sites. *Proceedings of the National Academy of Sciences*, 109(2):449–453, 2012.
- [5] W. Boomsma, K. V. Mardia, C. C. Taylor, J. Ferkinghoff-Borg, A. Krogh, and T. Hamelryck. A generative, probabilistic model of local protein structure. *Proceedings of the National Academy of Sciences*, 105:8932–8937, 2008.
- [6] W. Boomsma, K. V. Mardia, C. C. Taylor, J. Ferkinghoff-Borg, A. Krogh, and T. Hamelryck. A generative, probabilistic model of local protein structure. *Proceedings of the National Academy of Sciences*, 105(26):8932–8937, 2008.
- [7] P. J. A. Cock, T. Antao, J. T. Chang, B. A. Chapman, C. J. Cox, A. Dalke, et al. Biopython: freely available Python tools for computational molecular biology and bioinformatics. *Bioinformatics (Oxford, England)*, 25(11):1422–1423, 2009.
- [8] O. Faltinsen. *Sea loads on ships and offshore structures*, volume 1. Cambridge University Press, 1993.
- [9] J. J. Fernández-Durán and M. M. Gregorio-Domínguez. Modeling angles in proteins and circular genomes using multivariate angular distributions based on multiple nonnegative trigonometric sums. *Statistical Applications in Genetics and Molecular Biology*, 13(1):1–18, 2014.
- [10] J. J. Fernández-Durán and M. M. Gregorio-Domínguez. CircNNTSR: An R package for the statistical analysis of circular, multivariate circular, and spherical data using nonnegative trigonometric sums. *Journal of Statistical Software*, 70(6):1–19, 2016.
- [11] E. García-Portugués, M. Sørensen, K. V. Mardia, and T. Hamelryck. Langevin diffusions on the torus: estimation and applications. *Statistics and Computing*, 29:1–22, 2019.
- [12] C. Genest, K. Ghoudi, and L.-P. Rivest. A semiparametric estimation procedure of dependence parameters in multivariate families of distributions. *Biometrika*, 82(3):543–552, 1995.
- [13] V. Genna, A. Hospital, and M. Orozco. SARS-CoV-2 Inhibition, Host Selection and Next-Move Prediction Through High-Performance Computing, 2020.
- [14] T. Hamelryck, K. V. Mardia, and J. Ferkinghoff-Borg, editors. *Bayesian Methods in Structural Bioinformatics*. Springer, Heidelberg, Germany, 2012.
- [15] T. Harder, W. Boomsma, M. Paluszewski, J. Frellsen, K. E. Johansson, and T. Hamelryck. Beyond rotamers: a generative, probabilistic model of side chains in proteins. *BMC Bioinformatics*, 11:306, 2010.
- [16] G. Huang, A. W.-K. Law, and Z. Huang. Wave-induced drift of small floating objects in regular waves. *Ocean Engineering*, 38(4):712–718, 2011.
- [17] A. Jacobsen, E. van Dijk, H. Mouhib, B. Stringer, O. Ivanova, J. Gavaldá-García, et al. Introduction to Protein Structure. *arXiv*, 2307.02169, 2023.
- [18] S. R. Jammalamadaka and A. Sengupta. *Topics in Circular Statistics*. World Scientific, 2001.
- [19] H. Joe. *Multivariate Models and Multivariate Dependence Concepts*. Chapman and Hall/CRC, 1997.
- [20] H. Joe. *Dependence Modeling with Copulas*. CRC Press, Boca Raton, FL, USA, 2015.
- [21] R. A. Johnson and T. E. Wehrly. Some angular-linear distributions and related regression models. *Journal of the American Statistical Association*, 73(363):602–606, 1978.
- [22] M. C. Jones, A. Pewsey, and S. Kato. On a class of circulars: copulas for circular distributions. *Annals of the Institute of Statistical Mathematics*, 67:843–862, 2015.
- [23] W. Kabsch and C. Sander. Dictionary of protein secondary structure: Pattern recognition of hydrogen-bonded and geometrical features. *Biopolymers*, 22(12):2577–2637, 1983.
- [24] S. Kato, C. Ley, S. Loizidou, and K. V. Mardia. The trivariate wrapped cauchy copula. *arXiv*, 2401.10824, 2025.

- [25] S. Kato and A. Pewsey. A Möbius transformation-induced distribution on the torus. *Biometrika*, 102(2):359–370, 03 2015.
- [26] S. Kim, A. SenGupta, and B. C. Arnold. A multivariate circular distribution with applications to the protein structure prediction problem. *Journal of Multivariate Analysis*, 143:374–382, 2016.
- [27] F. Lagona, M. Picone, and A. Maruotti. A hidden Markov model for the analysis of cylindrical time series. *Environmetrics*, 26(8):534–544, 2015.
- [28] T. J. Lane. Protein structure prediction has reached the single-structure frontier. *Nature Methods*, 20(2):170–173, 2023.
- [29] C. Ley and T. Verdebout, editors. *Applied Directional Statistics: Modern Methods and Case Studies*. Chapman and Hall/CRC Press, Boca Raton, Florida, 2018.
- [30] K. V. Mardia. Statistical approaches to three key challenges in protein structural bioinformatics. *Journal of the Royal Statistical Society: Series C (Applied Statistics)*, 62:487–514, 2013.
- [31] K. V. Mardia. Fisher’s legacy of directional statistics, and beyond to statistics on manifolds. *Journal of Multivariate Analysis*, 207:105404, 2025.
- [32] K. V. Mardia, S. Barber, P. M. Burdett, J. T. Kent, and T. Hamelryck. Mixture Models for Spherical Data with Applications to Protein Bioinformatics. In A. SenGupta and B. C. Arnold, editors, *Directional Statistics for Innovative Applications: A Bicentennial Tribute to Florence Nightingale*, pages 15–32. Springer Nature, Singapore, 2022.
- [33] K. V. Mardia, G. Hughes, C. C. Taylor, and H. Singh. A multivariate von Mises distribution with applications to bioinformatics. *Canadian Journal of Statistics*, 36:99–109, 2008.
- [34] K. V. Mardia and P. E. Jupp. *Directional Statistics*. John Wiley & Sons, Chichester, United Kingdom, 2000.
- [35] K. V. Mardia and C. Ley. Directional distributions. In *Wiley StatsRef: Statistics Reference Online*, pages 1–13. John Wiley & Sons, Ltd, 2018.
- [36] K. V. Mardia, C. C. Taylor, and G. K. Subramaniam. Protein bioinformatics and mixtures of bivariate von Mises distributions for angular data. *Biometrics*, 63:505–512, 2007.
- [37] G. Mastrantonio. The joint projected normal and skew-normal: A distribution for poly-cylindrical data. *Journal of Multivariate Analysis*, 165:14–26, 2018.
- [38] A. Navarro, J. Frellsen, and R. Turner. The multivariate generalised von Mises distribution: inference and applications. *Proceedings of the Thirty-First AAAI Conference on Artificial Intelligence (AAAI-17)*, pages 2394–2400, 2017.
- [39] A. Pewsey and E. García-Portugués. Recent advances in directional statistics (with discussion). *TEST*, 30(1):1–58, 2021.
- [40] A. Pleskachevsky, D. P. Eppel, and H. Kapitza. Interaction of waves, currents and tides, and wave-energy impact on the beach area of Sylt Island. *Ocean Dynamics*, 59(3):451–461, 2009.
- [41] A. Selvitella. On geometric probability distributions on the torus with applications to molecular biology. *Electronic Journal of Statistics*, 13(2):2717 – 2763, 2019.
- [42] A. W. Senior, R. Evans, J. Jumper, J. Kirkpatrick, L. Sifre, T. Green, et al. Protein structure prediction using multiple deep neural networks in the 13th Critical Assessment of Protein Structure Prediction (CASP13). *Proteins: Structure, Function, and Bioinformatics*, 87(12):1141–1148, 2019.
- [43] C. B. Thygesen, C. S. Steenmans, A. S. Al-Sibahi, L. S. Moreta, A. B. Sørensen, and T. Hamelryck. Efficient Generative Modelling of Protein Structure Fragments using a Deep Markov Model. In *Proceedings of the 38th International Conference on Machine Learning*, pages 10258–10267. PMLR, 2021.
- [44] T. E. Wehrly and R. A. Johnson. Bivariate models for dependence of angular observations and a related Markov process. *Biometrika*, 66:255–256, 1980.